Surface and Bulk Tortuosity of Porous Ceramics near the Percolation Threshold

Miguel Bernard and Gary A. Williams
Physics Department, University of California, Los Angeles, California 90024
(Received 3 June 1991)

The surface and bulk tortuosities of sintered Al_2O_3 ceramic samples have been measured using third- and fourth-sound propagation in superfluid ^{4}He as a probe. Near the pore-space percolation threshold the index of refraction of both sound modes is found to increase rapidly as the porosity is lowered, to much higher values than previously observed. The bulk tortuosity exceeds the surface tortuosity for porosities below 30%, a reversal of the behavior observed at high porosity.

PACS numbers: 81.35.+k, 67.40.Hf, 67.40.Pm, 81.60.Dq

There is considerable interest in characterizing the structure of disordered materials. Transport properties of fluids in porous media are of fundamental interest, and also have practical applications [1]. By using superfluid ^{4}He as an acoustic probe we have measured the surface and bulk tortuosities of porous ceramic materials. We observe a dramatic divergence in the index of refraction of both third and fourth sound as the pore space in the samples is reduced by sintering. This divergence indicates the approach to the percolation threshold, the point where there is no longer a connected path across the sample. These techniques can allow an experimental test of recent theories of percolation in disordered systems [2].

Superfluid ^{4}He acoustics is an important tool for studying the properties of porous materials because the zero viscosity of the superfluid component allows sound propagation in fine pores where a classical fluid would be immobilized by viscous forces. The measured speed of sound of ^{4}He in the porous medium is reduced because of the tortuous path that the fluid is forced to follow through the connected pore spaces. The lowered speed is characterized by an index of refraction, which is the ratio of the theoretical speed in an ideal geometry (i.e., straight capillaries) to the experimentally measured speed. For the case of pores completely filled with superfluid ^{4}He where the normal fluid is viscously locked, the propagating low-frequency acoustical mode is known as fourth sound [3]. The theoretical speed of fourth sound is $c_4=(\rho_s/\rho)^{1/2}c_1$, where ρ_s/ρ is the bulk superfluid fraction and c_1 is the velocity of first sound. The fourth-sound index of refraction is then $n_4=c_4/c_{4\text{expt}}$. A similar index can be defined for the case when only a thin film of ^{4}He is adsorbed on the pore surface. The propagating mode in this case is third sound [3], a surface-height wave that is accompanied by temperature oscillations. The third-sound index of refraction is $n_3=c_3/c_{3\text{expt}}$, where

$$c_3^2=3\alpha\frac{\rho_s}{\rho}\left(\frac{d-D_0}{d^4}\right), \tag{1}$$

with d the thickness of the ^{4}He film, α the Van der Waals constant, and D_0 the thickness of the effective nonsuperfluid layer [4].

The index of refraction of fourth sound is related to the bulk tortuosity parameter α_{3D} of the Biot theory [5] of porous-media hydrodynamics by [6] $n_4^2=\alpha_{3D}$. Similarly, a surface tortuosity parameter α_{2D} can be defined [7] as $n_3^2=\alpha_{2D}$. In this Letter, we report the first systematic measurements of both α_{3D} and α_{2D} in the same sample as a function of the sample porosity ϕ, where ϕ is the ratio of pore volume to total volume. As remarked above, we find that both tortuosities increase rapidly close to the pore-space percolation threshold, to much higher values than have been observed previously. In the low-porosity regime, α_{3D} is found to exceed α_{2D}, a reversal of the behavior at high porosities [8,9].

Our samples are sintered Al_2O_3 ceramics prepared using a slip-casting [10] technique and firing in an oven. Al_2O_3 powder, of 500-Å nominal grain size [11], and water are mixed for about 4 h in the ratio 2:1 by weight. A small amount of HCl is added to maintain a pH of 3 for better mixing, yielding a homogeneous slurry that is then poured into a plaster of Paris mold. The mold removes the water, leaving behind a casting of the powder having a porosity between 52% and 60%. The cast is dried at 140 °C for 12 h and then can be machined into several samples of regular shape (rectangular or cylindrical). Each sample is then sintered in a furnace for about 90 min at temperatures ranging from 1350 to 1650 °C. This results in samples having a range of final porosities between 50% and 6%. Porosity is measured by weighing the samples and measuring their dimensions, a technique which includes completely blocked-off pore spaces. This was checked for several samples by measuring the volume of liquid helium needed to just fill the pores, and this yielded the same porosity to within a few percent. Electron microscope pictures of the sample surfaces show an increasing grain size with decreasing porosity, as seen in Fig. 1. The grain size is about 0.5 μm in the 30% sample, increasing to $\sim$4 μm in the 6.7% sample.

Each sintered sample is then epoxied with Stycast 2850 GT [12] into a brass cylinder whose length is machined to match the sample length. Each end of the cylinder is sealed (using an indium O-ring) by a transducer cap that mounts flush to the ceramic surface. For third-sound measurements, the drive transducer is a heater film of resistive carbon paint of resistance about 50 Ω. The pickup transducer is a current-biased 200-Ω $\frac{1}{8}$-W Allen-Bradley resistor with the insulating case partially

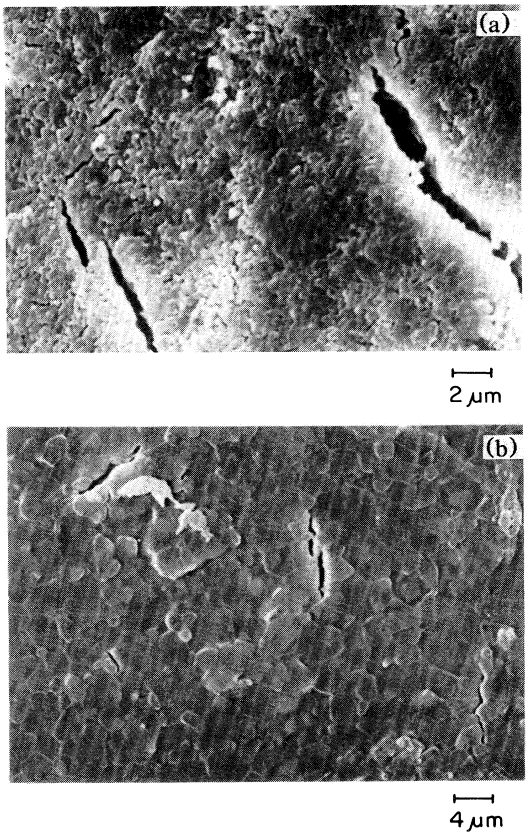

FIG. 1. Scanning transmission electron microphotographs of the surface of two sintered samples. (a) 30.3% porosity and (b) 6.7% porosity.

sanded off. For fourth sound, aluminized Teflon electret transducers are used as the pickup and the drive.

The experimental speed of each sound mode is determined from the resonant mode frequencies and the sample dimensions. A slow sweep of the drive frequency is carried out while the resonant response is monitored using a fast Fourier-transform analyzer in an averaging mode. For third sound, the adsorbed helium film thickness is determined using the standard Frankel-Halsey-Hill isotherm [3], as in previous studies using Al_2O_3 powders [13]. A value $\alpha = 31$ K (layers)^3 is used, taking an atomic layer to be 3.6 Å. Figure 2 shows the measured third-sound speeds versus film thickness for four samples of different porosity. The measurements cut off at thin films because of the high attenuation near the Kosterlitz-Thouless critical thickness [13]; for the lowest-porosity samples an anomalously low Q factor makes the signal observable only at thicker films.

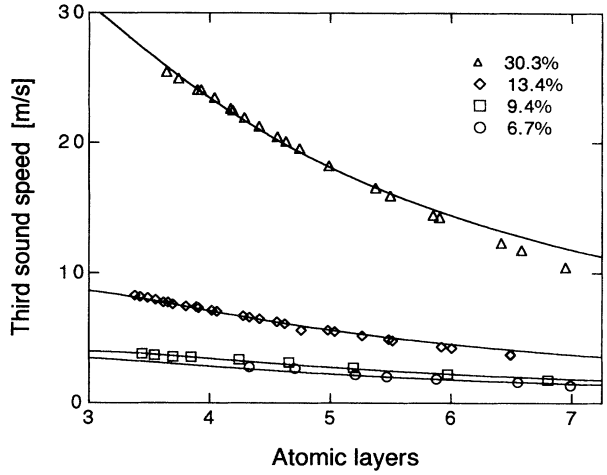

FIG. 2. Third-sound speeds for samples of four different porosities as a function of ^{4}He film thickness, at constant temperature $T = 1.37$ K. The solid lines are fits by Eq. (1).

The striking characteristic of the third-sound data is the rapid decrease of c_{expt} as the sample porosity decreases. The index of refraction is extracted from this data by fitting with Eq. (1), varying n_3 and D_0, shown as the solid lines in Fig. 2. The results are tabulated in Table I, and n_3 is shown as the circles in Fig. 3. There is a considerable increase in the index as the porosity is lowered.

Fourth-sound measurements were carried out on the same sample set, and the resulting values of n_4 are shown

TABLE I. Characteristics of the sample set shown in Fig. 3, which had an initial slip-cast porosity of 53.8%. The value used for the density of Al_2O_3 is 3.96 g/cm^3.

Porosity (%)	Sintering temperature (°C)	Total volume (cm^3)	Surface area / Weight (m^2/g)	D_0 $T = 1.37$ K (atomic layers)	n_3	n_4
6.7 ± 0.1	1600	0.60 ± 0.02	0.98 ± 0.05	2.10	13.0	26.7
9.4 ± 0.1	1570	0.50 ± 0.02	0.67 ± 0.05	2.26	10.27	17.1
13.4 ± 0.1	1500	0.45 ± 0.02	2.00 ± 0.08	2.12	5.15	8.3
30.5 ± 0.1	1350	0.78 ± 0.02	2.85 ± 0.08	1.81	1.68	2.7
52.3 ± 0.5 [a]	unsintered	0.14	59	···	1.55	1.36

[a]Data taken by Beamish with the techniques described in Ref. [24]. This sample was from a different slip casting, but had nearly the same initial porosity as the other samples.

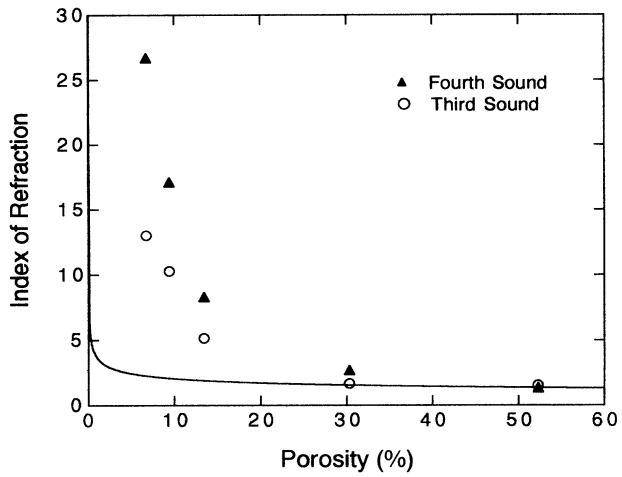

FIG. 3. Index of refraction for third and fourth sound as a function of sample porosity, for the sample set of Table I. The solid line is Eq. (2) with $m=\frac{3}{2}$ and $a=1.34$.

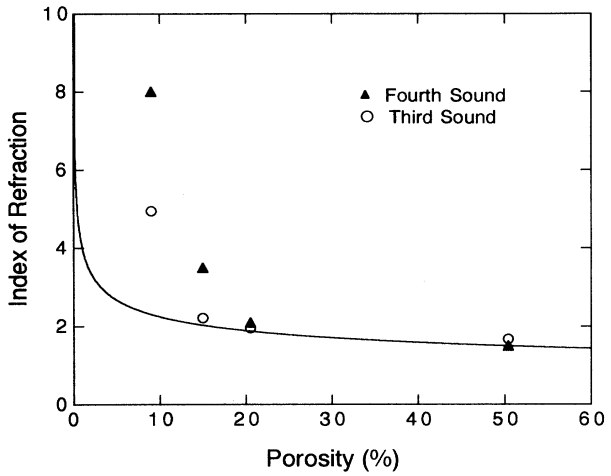

FIG. 4. Index of refraction vs porosity for a second set of samples. The solid line is Eq. (2) with $m=\frac{3}{2}$ and $a=1.60$.

as the triangles in Fig. 3. The fourth-sound index is considerably larger than the third-sound index for porosities below 30%. The value of $n_4=26.7$ in the 6.7% sample is much larger than seen in any previous fourth-sound studies in porous materials [14]. The solid line in Fig. 3 is Archie's law [15,16]

$$\alpha_{3D}=n_4^2=a\phi^{-m+1}, \tag{2}$$

which was found to fit previous measurements [17–19] of α_{3D} at higher porosities. Superfluid measurements [17] of α_{3D} in $\sim$200-μm sintered glass beads were found to be described by $m=\frac{3}{2}$ and $a=1$ for porosities above 20%; the line in Fig. 3 uses the same m but takes $a=1.34$ to match the index in the 52.3% sample. It is clear that our data for both n_3 and n_4 deviate strongly from Eq. (2) at low porosities. Very similar behavior was observed in another set of samples with porosity ranging between 50% and 9%, shown in Fig. 4. The set of Fig. 4 had an initial slip-cast porosity of 57%, less dense than the 53.8% initial porosity of the samples of Fig. 3. Again, n_4 is larger than n_3 below $\sim$30% porosity, although both values are not as high as in Fig. 3.

The rapid increase observed for both α_{3D} and α_{2D} with decreasing porosity is most likely connected with the approach to the pore-space percolation threshold in these materials. Various estimates [20,21] of the percolation threshold in sintered materials are in the porosity range of 2%–5%. Archie's law must break down in this regime, since it does not account for the finite threshold porosity ϕ_c. A number of theoretical models [2,21,22] suggest instead that the tortuosities should vary as a power law of $\phi-\phi_c$,

$$\alpha_{2D,3D}=a'\phi(\phi-\phi_c)^{-\bar{t}}, \tag{3}$$

where a' is a constant and the exponent $\bar{t}$ has been identified [2] as the electrical conductivity exponent for percolation in disordered continuum systems. Feng, Halperin, and Sen [2], using a random Swiss cheese model, estimate values of $\bar{t}=1.3$ in 2D and $\bar{t}=2.4$ in 3D. Although we do not have a sufficient number of data points in the percolation regime to extract these exponents, our data are at least in qualitative agreement with the prediction that α_{3D} should increase faster than α_{2D}. There have also been numerical simulations [21,23] using truncated sphere models that predict α_{3D} to exceed α_{2D}. For growing spheres constrained by the cells of a cubic lattice, where ϕ_c is at 3.5%, the 3D tortuosity becomes larger than the 2D tortuosity only at porosities below 4.4% [23]. Our data, however, show α_{3D} to be dominant over a much larger range of porosity than this.

The initial porosity of the slip casting appears to be an important parameter: Both tortuosities depend not just on the final sintered porosity of the sample, but also on the initial porosity. The data sets in Figs. 3 and 4 do not fall on the same curves; the data in Fig. 3 are consistently higher, by as much as a factor of 2, than those of Fig. 4 at the same porosity. This may be the result of a different percolation threshold between the two sample sets, with a higher threshold for the samples of Fig. 3 due to the denser initial slip casting.

A surprising feature of the experiments was the observation of significant dissipation in the samples of lowest porosity. For example, the 6.7% sample had a third-sound Q factor of 7 at 4.6 layers, compared to a Q of over 200 in the 30.3% sample at similar thicknesses. The fourth-sound Q in the 6.7% sample at 1.65 K was 30, compared to $\sim10^3$ in the 30.3% sample. This does not seem to be viscous damping that could arise from an increase in pore size, since the third-sound mode should be unaffected by pore size. At high drive levels a nonlinear shift in the resonant frequency to lower values was ob-

served, a phenomenon not seen in high-porosity samples.

In summary, we have measured the surface and bulk tortuosities of sintered ceramic samples at porosities approaching the percolation threshold. In these exploratory measurements a divergence of the tortuosities is observed as the threshold is approached. The ^{4}He sound propagation measurements are a sensitive probe of the structure of these disordered materials, and further experiments can now be designed. A determination of the percolation exponents will require a more extensive sample set covering a narrower range near the threshold.

This work is supported in part by the National Science Foundation, Grant No. DMR 89-12825. We are grateful to R. Chu, J. P. Desideri, F. Gallet, and K. J. Gurfield for sample development and preparation, C. Hayase and B. Ruff for taking initial fourth-sound data, and J. R. Beamish for the unsintered sample measurements. We have benefited from discussions with S. Feng, D. L. Johnson, R. Pober, S. Putterman, and L. M. Schwartz.

[1] J. P. Clerc, G. Giraud, J. M. Laugier, and J. M. Luck, Adv. Phys. **39**, 191 (1990); P. Wong, Phys. Today **41** (12), 24 (1988).
[2] S. Feng, B. I. Halperin, and P. N. Sen, Phys. Rev. B **35**, 197 (1987).
[3] S. J. Putterman, *Superfluid Hydrodynamics* (North-Holland, Amsterdam, 1974).
[4] J. H. Scholtz, E. O. McLean, and I. Rudnick, Phys. Rev. Lett. **32**, 147 (1974).
[5] M. A. Biot, J. Acoust. Soc. Am. **28**, 168 (1956).
[6] D. L. Johnson, Appl. Phys. Lett. **37**, 1065 (1980).
[7] D. L. Johnson, T. J. Plona, and H. Kojima, in *Physics and Chemistry of Porous Media II—1986,* edited by J. R. Banavar, J. Koplik, and K. W. Winkler, AIP Conference Proceedings No. 154 (American Institute of Physics, New York, 1987), p. 243.
[8] S. Baker, J. Marcus, G. A. Williams, and I. Rudnick, in *Physics and Chemistry of Porous Media I—1983,* edited by D. J. Johnson and P. N. Sen, AIP Conference Proceedings No. 107 (American Institute of Physics, New York, 1984), p. 119.
[9] R. Rosenbaum *et al.*, J. Low Temp. Phys. **37**, 663 (1979).
[10] W. J. Kingery, *Introduction to Ceramics* (Wiley, New York, 1960).
[11] Linde B UCAR Alumina Powder, Union Carbide Corporation, 1550 Polco Street, Indianapolis, IN 46224.
[12] Emerson & Cuming, W. R. Grace & Co., Canton, MA 02021.
[13] V. Kotsubo and G. A. Williams, Phys. Rev. B **33**, 6106 (1986).
[14] J. A. Roth, T. P. Brosuis, and J. D. Maynard, Phys. Rev. B **38**, 11 209 (1988).
[15] G. E. Archie, Trans. Metall. Soc. AIME **146**, 54 (1942).
[16] P. N. Sen, C. Scala, and M. H. Cohen, Geophysics **46**, 781 (1981).
[17] D. L. Johnson, T. J. Plona, C. Scala, F. Pasierb, and H. Kojima, Phys. Rev. Lett. **49**, 1840 (1982).
[18] P. Wong, J. Koplik, and J. P. Tomanic, Phys. Rev. B **30**, 6606 (1984).
[19] F. Brouers and A. Ramsamugh, Solid State. Commun. **60**, 951 (1986).
[20] W. T. Elam, A. R. Kerstein, and J. J. Rehr, Phys. Rev. Lett. **52**, 1516 (1984).
[21] J. N. Roberts and L. M. Schwartz, Phys. Rev. B **31**, 5990 (1985).
[22] P. N. Sen, W. C. Chew, and D. Wilkinson, in *Physics and Chemistry of Porous Media I* (Ref. [8]), p. 52.
[23] D. L. Johnson and L. M. Schwartz (to be published).
[24] K. L. Warner and J. R. Beamish, Phys. Rev. B **36**, 5698 (1987).

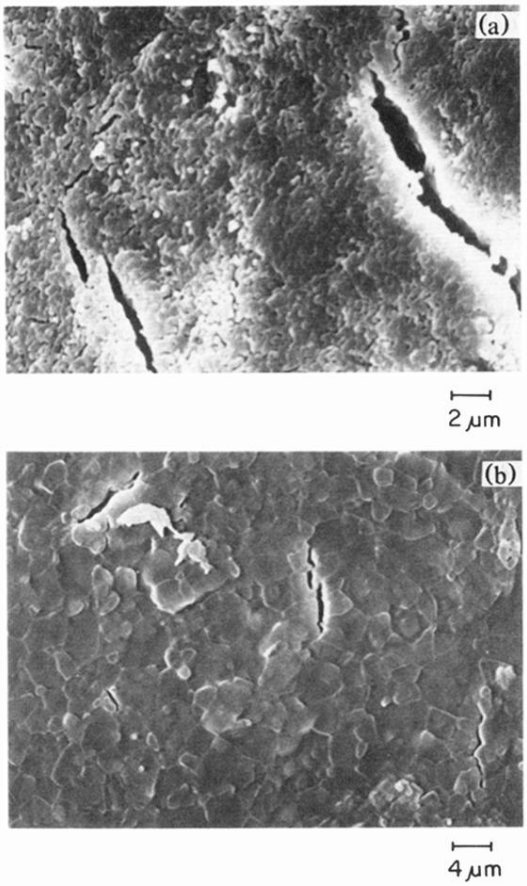

FIG. 1. Scanning transmission electron microphotographs of the surface of two sintered samples. (a) 30.3% porosity and (b) 6.7% porosity.